

The role of periodic orbits and bubbles of chaos during the transition to turbulence

S. Altmeyer^{1†},
A. P. Willis² and B. Hof¹

¹Institute of Science and Technology Austria (IST Austria), 3400 Klosterneuburg, Austria

²School of Mathematics and Statistics, University of Sheffield, Sheffield S3 7RH, UK

(Received ?; revised ?; accepted ?. - To be entered by editorial office)

Starting with turbulence that explores a wide region in phase space, we discover several relative periodic orbits (RPOs) embedded within a subregion of the chaotic turbulent saddle. We also extract directly from simulation, several travelling waves (TWs). These TWs together with the RPOs are unstable states and are believed to provide the skeleton of the chaotic saddle. Earlier studies have shown that such invariant solutions can help to explain wall bounded shear flows, and a finite subset of them are expected to dominate the dynamics (Faisst & Eckhardt 2003; Pringle & Kerswell 2007; Hof *et al.* 2004). The introduction of symmetries is typically necessary to facilitate this approach. Applying only the shift-reflect symmetry, the geometry is less constrained than previous studies in pipe flow. A ‘long-period’ RPO is identified that is only very weakly repelling. Turbulent trajectories are found to frequently approach and frequently shadow this orbit. In addition the orbit characterises a resulting ‘bubble’ of chaos, itself a saddle, deep within the turbulent sea (Kreilos *et al.* 2014). We explicitly analyse the merger of the two saddles and show how it results in a considerable increase of the total lifetime. Both *exits and entries* to the bubble are observed, as the stable manifolds of the inner and outer saddles intertwine. We observe that the typical lifetime of the turbulence is influenced by switches between the inner and outer saddles, and is thereby dependent on whether or not it ‘shadows’ or ‘visits’ the vicinity of the long-period RPO (Cvitanović *et al.* 2014). These observations, along with comparisons of flow structures, show that RPOs play a significant role in structuring the dynamics of turbulence.

Key words:

1. Introduction

??

Several families of exact coherent structures, i.e. invariant sets of solutions, have been identified in plane Couette flow (Nagata 1990; Jiménez *et al.* 2005), plane Poiseuille flow (Waleffe 2001, 2003), square duct flow (Wedin *et al.* 2009; Okino *et al.* 2010) and the geometry discussed here, pipe flow (Wedin & Kerswell 2004; Pringle & Kerswell 2007; Faisst & Eckhardt 2003). In general, the state space is filled with a multitude of unstable invariant solutions that are explored by turbulent trajectories. At low flow rates the trajectory eventually escapes from the roller coaster ride through this neighbourhood and ends on the steady laminar attractor, turbulence is transient here and the turbulent

† Email address for correspondence: sebastian.altmeyer@t-online.de

neighbourhood corresponds to a *chaotic saddle* (Kreilos *et al.* 2014). In a circular pipe, the laminar Hagen–Poiseuille flow is linearly stable at all Reynolds numbers ($Re = DU/\nu$, where D is the pipe diameter, U the mean axial velocity and ν the kinematic viscosity of the fluid). Several families of three-dimensional travelling wave (TW) solutions have been discovered (Faisst & Eckhardt 2003; Wedin & Kerswell 2004), which represent the ‘simplest’ invariant solutions in pipe flow satisfying

$$\mathbf{u}(r, \theta, z, t) = \mathbf{u}(r, \theta, z - ct), \quad (1.1)$$

where (r, θ, z) are the usual cylindrical coordinates, $\mathbf{u} = (u, v, w)$ are the corresponding velocity components, t the time and c the wave speed. The TW solutions originate from saddle-node bifurcations at a finite value of the Reynolds number. Mellibovsky and Eckhardt (Mellibovsky & Eckhardt 2011) provide a fundamental study of TWs’ origins and their subsequent varied bifurcations. Periodic solutions on the other hand bifurcate classically in a Hopf bifurcation out of TWs. Orbits are important as they capture the dynamics. In a recent study of transition in Couette flow, Kreilos and Eckhardt (Kreilos & Eckhardt 2012), found that such orbits undergo a transition sequence to chaos. They followed the bifurcation of exact coherent states that undergo period-doubling cascades and end with a crisis bifurcation. Due to the strong advection of structures in pipe flow, only ‘relative’ periodic orbits (RPOs) are observed. These orbits include a streamwise translation with mean phase speed \bar{c} . Of these, only few have been discovered so far (Duguet *et al.* 2008; Willis *et al.* 2013; Avila *et al.* 2013). They are expected to capture the natural measure of turbulent flow (Cvitanović & Gison 2009; Willis *et al.* 2013). Such RPOs satisfy

$$\mathbf{u}(r, \theta, z, t) = \mathbf{u}(r, \theta, z - \bar{c}t, t + T), \quad (1.2)$$

such that the motion appears T -periodic in a frame co-moving at speed \bar{c} . The value \bar{c} is different for each RPO. Similar structures were also reported in plane Couette flow (Kawahara & Kida 2001; Kawasaki & Sasa 2005; Viswanath 2007). To date, the number of RPOs discovered in pipe flow is few and all searches were limited to subspaces with rotational symmetries (Mellibovsky & Eckhardt 2011; Willis *et al.* 2013). It is worth mentioning, however, that any solution found in a subspace are necessarily also solutions of the full space and hence represent physically consistent flow states. All RPOs discovered were embedded in regions of ‘lower’ energy (below turbulent levels) but it was speculated that RPOs at higher energy levels exist that underpin the dynamics of turbulence.

All known invariant solutions other than the laminar flow are unstable at the Reynolds numbers for which turbulence is observed, but the dimensions of their unstable manifolds in phase space is typically low (Kawahara 2005; Kerswell & Tutty 2007; Waleffe 2001; Viswanath 2009). Hence it is expected that they can be approached closely along their stable manifolds. The least unstable orbits are expected to be the most representative, and are the most likely to be extracted from simulation.

In this paper we isolate and link significant features of turbulent dynamics to several representative RPOs, including one with a much longer period time than previously computed orbits. We present results of invariant solutions for a ‘minimal’ practical set of symmetry, imposing only shift-reflect and no rotational symmetry. When the long-period RPO emerges it forms a localised bubble of chaos within the rest of turbulence. Shadowing, or ‘visits’ to this invariant solution significantly increase the turbulent lifetime. The resulting lifetime of a trajectory is dependent on the rate of switching, that is, we observe ‘entries’ and ‘exits’ from the bubble. In addition, the long-period RPO captures much of the qualitative features of turbulence, including streak break-up and repetitions in chaotic trajectories.

2. Numerics and Formulation

To find invariant states we first apply the symmetry reduction *method of slices* (Willis *et al.* 2013; Budanur *et al.* 2014) to pipe flow to obtain a quotient of the streamwise translation symmetry of turbulent flow states. Within the symmetry-reduced state space, all TWs reduce to equilibria and all RPOs reduce to periodic orbits. The method bypasses the difficulties of \bar{c} being different for each RPO in an automatic manner, and permits much simpler identification and extraction of TWs and RPOs directly from turbulent chaotic trajectories. For simulations we use a hybrid spectral finite-difference code (Willis & Kerswell 2009) with 64 non-equispaced finite difference axial points, Fourier expansions evaluated on 48 azimuthal points and on 24 points per unit radius in the radial direction (idealised). The shift-reflect symmetry, carried by almost all known TWs, is applied,

$$\mathbf{S} : (u, v, w)(r, \theta, z, t) = (u, -v, w)(r, -\theta, z, t). \quad (2.1)$$

For convergence and continuation of solutions we used a Newton-Krylov-hookstep algorithm (Viswanath 2007) with minor enhancements in adjustments to the norm (Willis *et al.* 2013). The relative residual of the RPOs is at least approximately 10^{-7} for the longest orbit, and is considerably less ($< 10^{-8}$) for the others. While we have not imposed further symmetries, some of the observed TW solutions are highly-symmetric N1 (Pringle *et al.* 2009), which also satisfy shift-and-rotate symmetry

$$\mathbf{\Omega} : (u, v, w)(r, \theta, z, t) = (u, v, w)(r, \theta + \pi, z - \pi/\alpha, t), \quad (2.2)$$

where $2\pi/\alpha$ ($\alpha = 1.25$) is the wavelength. (See (Willis *et al.* 2013) Appendix regarding relationships between symmetries in pipe flow.) For the present work we fixed $Re = 2300$ and have chosen a domain of length $5D$, which is a compromise between the reduced computational expense of a smaller domain and the need for the pipe to be sufficiently long to accommodate turbulent dynamics. We note that it has recently been shown that the key features of localised TWs are easily encompassed within a domain of similar length in pipe flow (Chantry *et al.* 2014). For these parameters, turbulence is found to be transient with characteristic life-time $\bar{t} \approx 10^3 D/U$.

3. Relative Periodic Orbits

The classical physical quantities, input energy $I = V^{-1} \oint dS[\mathbf{n} \cdot \mathbf{u}]p$, dissipation $D = \|\nabla \times \mathbf{u}\|_2^2/Re$ and the kinetic energy $E = \|\mathbf{u}\|_2^2/2$, where $\|\cdot\|$ corresponds to a root-mean-square value, are often used for phase space representation. Figure 1 presents projections of several travelling waves and the relative periodic orbits. For notation we follow the works (Kerswell & Tutty 2007; Pringle *et al.* 2009). Highly-symmetric TWs with both shift-reflect and shift-rotate symmetry (S, Ω) are named ‘N1’, and states with only shift-reflect symmetry (S) are called ‘S1’. We identify different RPOs with subscript corresponding to their period. (Note that these numbers refer to $Re = 2300$ and change with Re (Willis *et al.* 2013).) Due to energy balance, all TWs, time-averages of RPOs and a sufficiently long time-average of a turbulent flow must lie on the diagonal $D = I$ (see Fig. 1(a)). While the lower branch travelling waves N1L and S1L (see Fig. 1(a)) are far from the turbulent flow, the TWs, N1M2 and N1U appear to be in the core of the turbulent region (Although the classes ‘N’ and ‘S’ are well known most of ‘1-fold’ solutions observed here are new.) Notably, all RPOs extracted from turbulent trajectories also lie within this region (in particular near the upper branch TW of N1U) while all short RPOs are enclosed by the long-period RPO_{72.001} in the energy plot (see Fig. 1(c)). Extraction of these orbits from simulation implies that they are among the least unstable, and are

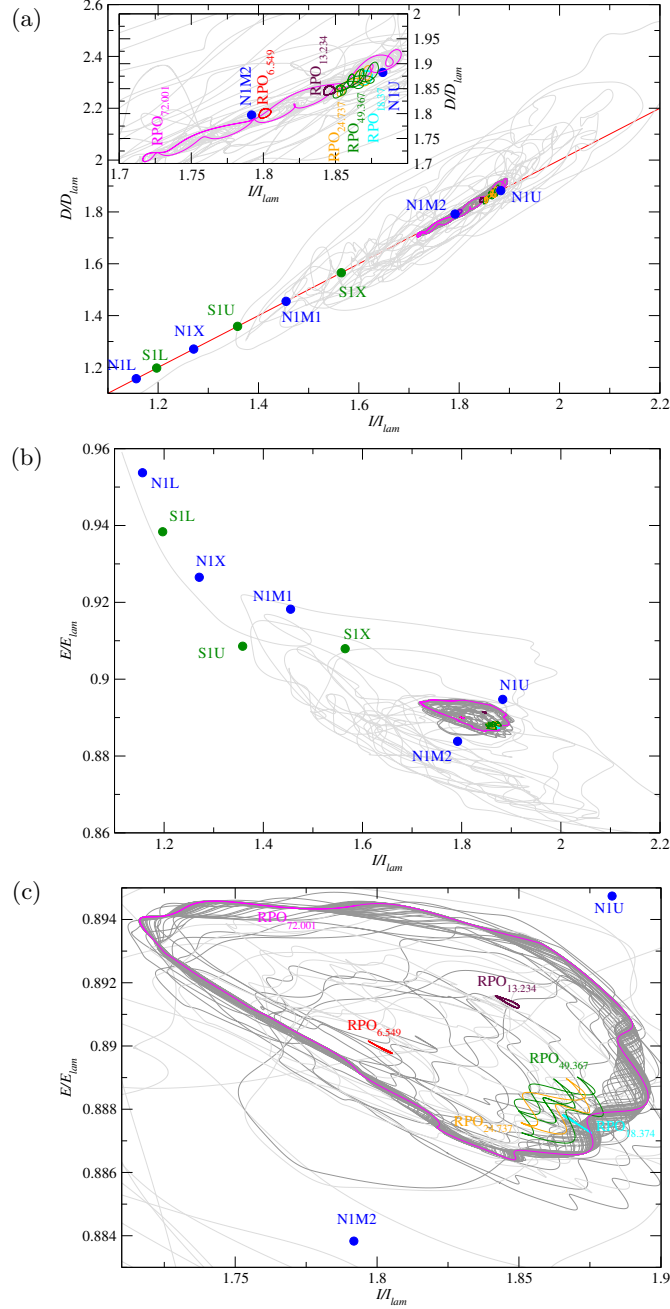


FIGURE 1. Rate of energy input from the background pressure gradient I (external power to maintain constant flux) versus (a) the dissipation rate D and (b) the energy E for the invariant solutions of TWs and RPOs, together with two turbulent orbits. (All quantities are normalised by their laminar counterparts.) Light gray presents a typical turbulent orbit while dark gray indicates orbits that shadow RPO_{72.001} and enter and exit the bubble. (c) and inset in (a) show an expanded view of the region near N1M2 and N1U where all here discovered RPOs are embedded. Note, due to visibility a full relaminarisation trajectory is only given for one simulation.

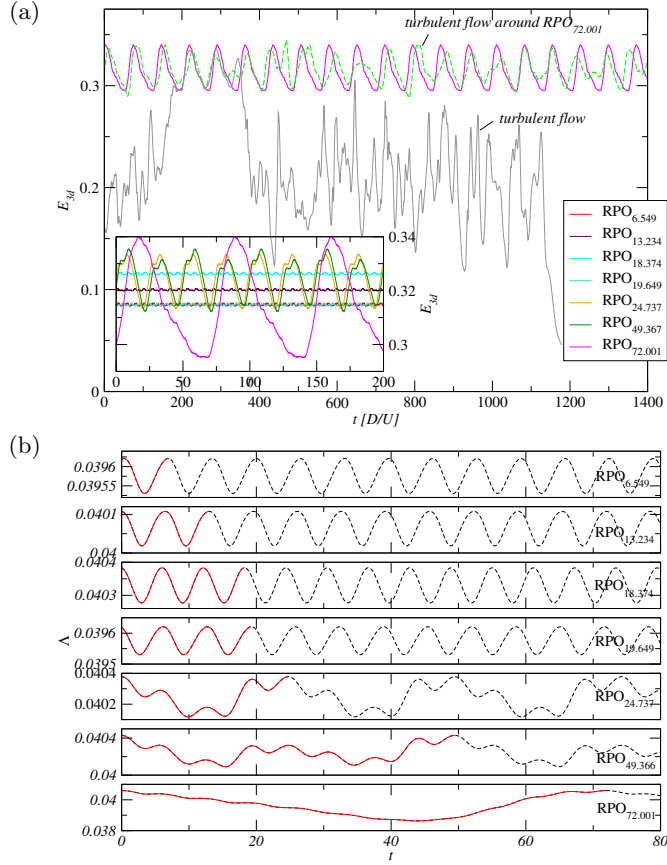


FIGURE 2. Dynamics of pipe flow for several RPOs and two turbulent runs. For the latter, one (green (dark gray) dashed) hangs around the long-period RPO_{72.001} (stuck in inner saddle) while the other shows a typical visit of the RPO_{72.001} orbit (here about two periods; typically about two to five periods) before it relaminarizes. (a) Energy E_{3d} versus time $t[D/U]$ for each RPO. The inset shows the periodic oscillation of all RPOs discussed in this letter. (b) Friction of RPOs as indicated. One cycle of each period is shown red (light gray) solid, with continuation black dashed.

therefore expected to be important and potentially representative of turbulent flow. In particular the long-period RPO_{72.001} is found to be dynamically relevant. Trajectories that happen to approach the orbit tend to stay close to it and encircle it (see dark regions in Fig. 1) for extended periods. This results in an overall increase in lifetimes. All RPOs discussed here lie in the core region, associated with higher dissipation, and underline their potential role as organising centers of the turbulent dynamics. In particular our RPOs are located near the solutions of upper branch TWs, rather than the lower branch TWs, the latter of which are more closely linked to transition.

Figure 2 illustrates the close correspondence between the dynamics of turbulent runs and those of RPO_{72.001}. Monitoring the energy $E_{3d} = \|\mathbf{u} - \bar{\mathbf{u}}\|_2^2/2$ (top panel), where $\bar{\mathbf{u}}$ is the axially averaged flow, and friction $\Lambda =: 2DG/\rho U^2$ (where G is the mean pressure gradient along the pipe and the density) (bottom panel) against time t we show and example trajectory (green, dashed) that stays around the long-period RPO_{72.001} for a very long time, and another (gray) that shows a more typical ‘visit’ to RPO_{72.001}, here for approximately two periods. The group of periodic orbits is shown in the inset

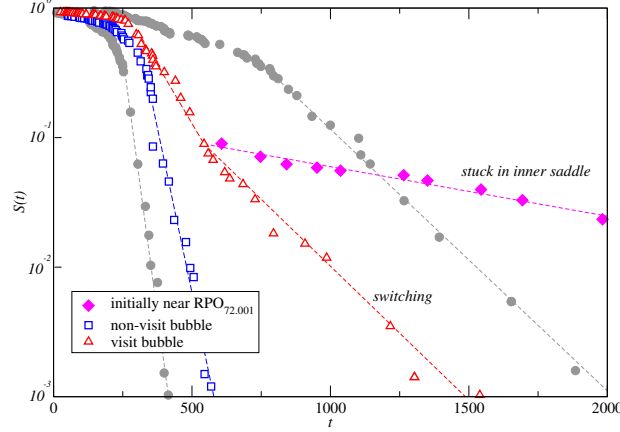


FIGURE 3. (a) Relaminarisation times of turbulent flows at $Re = 2300$ as a function of initial conditions (times in D/U) separated if its trajectories visit (\triangle) and non-visit (\square) the vicinity of $RPO_{72.001}$ orbit (horizontal dashed lines present averaged lifetimes) and initials near that orbit (\blacklozenge) which get stuck in the inner saddle. (b) Corresponding survivor function $S(t) = \exp[(t-t_0)/\tau_{\text{true}}]$, with $\tau_{\text{true}} = 1/r[\sum_{i=1}^r t_i + (n-r)t_r]$ (lifetime sample of size n with truncation after r decays) (Avila *et al.* 2010). The attractor of $RPO_{72.001}$ cause an offset to ‘nearby’ initial conditions that decay after longer times. ‘Switching’ refers to changes between inner and outer saddle. For comparison, results for $Re = 2250$ and $Re = 2450$ are also shown, which are below and above the range existing where $RPO_{72.001}$ exists ($2292 \lesssim Re(RPO_{72.001}) \lesssim 2423$).

of Fig. 2(a) and (b). The frequency of the shortest orbit $RPO_{6.549}$ appears as a fast frequency modulation of the longer period orbits. Closeness of the two orbits $RPO_{24.737}$ and $RPO_{49.367}$ is clear in both energy and friction (Fig. 2) and in the phase-space plot (Fig. 1). Compared to RPOs found by numerical continuation from bifurcations, the range of energy variation ΔE_{3d} is large (Willis *et al.* 2013), and the long period orbit $RPO_{72.001}$ explores a wide area deep in the turbulent sea (Fig. 1(b)). The orbits with the three next longer periods only show a week longer period modulation on top of the fast frequency. The three orbits with largest periods are modulated much more strongly. Equally they explore a wider range covered by the turbulent trajectories. Construction of orbits from shorter ones, and that longer orbits show rather complex structural changes and explore a wider range, supports the idea that RPOs function as building blocks of the turbulent motions. While $RPO_{24.737}$ and $RPO_{49.366}$ show several local maxima over one period, the longer $RPO_{72.001}$ is only very weakly modulated (one single peak, slowly varying over one full period). Independent of their period time, all these RPOs show the same underlying short-time modulation with approximately the period of the shortest one $RPO_{6.549}$ (Fig. 2(b)). Here it seems likely that all RPOs discussed may be members of the same family.

To quantify the effect of the bubble we calculated relaminarisation times of turbulent flows for about 300 initial conditions (ICs). These were separated in terms of those that ‘visit’ transiently the inner saddle or ‘bubble’ near $RPO_{72.001}$, and other trajectories which ‘non-visit’. The ‘bubble’ near $RPO_{72.001}$ is a saddle within the outer turbulent saddle that is sufficiently large to cover the dark gray region in Fig. 1. Large fluctuations in the data indicate that the ICs have uncorrelated lifetimes, but the lifetimes are longer for turbulent flows that visit the bubble. Based on these ICs we calculated the corresponding survivor functions $S(t)$ (Fig. 3). The exponential distribution $S(t) = \exp[(t-t_0)/\tau_{\text{true}}]$ estimate the characteristic turbulent lifetimes with the sample mean, which is the maximum likelihood estimator (MLE) of the parameter τ_{true} . ICs started in the very close

neighbourhood of the orbit $\text{RPO}_{72.001}$ spend very long time within this subregion (labelled ‘stuck in inner saddle’), but are otherwise uncorrelated. While their distribution follows that of a memoryless process, their long period results in distribution that is almost the superposition of an exponential and a constant, similar to the observation in (Kreilos *et al.* 2014), suggesting that they are associated with a further saddle within the inner saddle (or another ‘bubble’ within the bubble). More typically, all other ICs lead to trajectories that visit the bubble near $\text{RPO}_{72.001}$ for two to five periods, and the extended lifetime is dependent on the rate of ‘switching’, or ‘entries’ and ‘exits’ from the bubble.

Comparing before and after the range where the long period orbit $\text{RPO}_{72.001}$ exists ($2292 \lesssim Re(\text{RPO}_{72.001}) \lesssim 2423$) in Fig. 3 (gray circles), it is observed that at slightly higher $Re = 2450$ the flow has inherited the longer lifetime associated with the bubble (compare with slope for the ‘switching’ case). The bubble has fully merged with the outer saddle so that the spuriously long lifetimes associated with the possible saddle within in the inner saddle, no longer feature.

Our simulations highlight that visits, or ‘switches’, to the ‘bubble’ near $\text{RPO}_{72.001}$ are typically of around two to five period times, i.e. ‘shadowing’ this orbit two to five times, see Fig. 2(a). Thus visiting the bubble strongly affects the turbulent lifetimes suggesting that the RPOs that structure this region play a key role in the evolution of the turbulent flow. Notably also, perturbations of the shorter RPOs results in a turbulent flow that also remain in this region and around $\text{RPO}_{72.001}$ for substantial times. This strongly suggests further ‘shadowing’ of the orbits, and that longer orbits may be constructed in terms of shorter ones.

Figure 4 depicts a full cycle of the temporal evolution of spatial structures for $\text{RPO}_{72.001}$ and a turbulent flow in its neighbourhood in dark region in Fig. 1. The vortex structures given by isosurfaces of streamwise vorticity ω_z (constant value for all snapshots of 60% of its maximum) show significant variation over one period of $\text{RPO}_{72.001}$. While at the low energy point of the cycle (see point (a) in phase space plots) the shape is quite smooth with moderate vorticity. It significantly increases during the cycle at higher energy levels (b) (see also online available material), then structure breaks up (c). There is clear correspondence between the vortex structures of $\text{RPO}_{72.001}$ and the turbulent flows nearby. For both cases one observes the same formation sequence that changes from a streamwise vortex-dominant shape to the form of low-velocity streaks dominating the structure (see movie1.avi). This supports the notion that RPOs can encompass much of the structure and dynamics of turbulent flows.

4. Conclusion

In summary, applying a minimal set of symmetry we have discovered exact coherent solutions of the Navier-Stokes equations in pipe flow and extracted RPOs directly from turbulent velocity fields. We have discovered an RPO with long-period period of $72.001 D/U$, much longer than previously discovered in pipe flow and comparable shear flows. The ‘bubble’ around the orbit is a chaotic saddle within the wider saddle of turbulence, and supports the idea that bubbles of chaos continue to have and influence *after* the crisis bifurcation (Kreilos & Eckhardt 2012). Here, the stable manifold of inner and outer saddles are observed to be highly intertwined, resulting in entry and exit to the bubble. At the initially chosen parameters we were able to observe the switching process clearly, while from lower to higher Re we have calculated that there is an increase in the mean lifetime. Trajectories that visit the bubble have significantly longer characteristic lifetimes than those that do not appear to visit this region, and we have seen that the

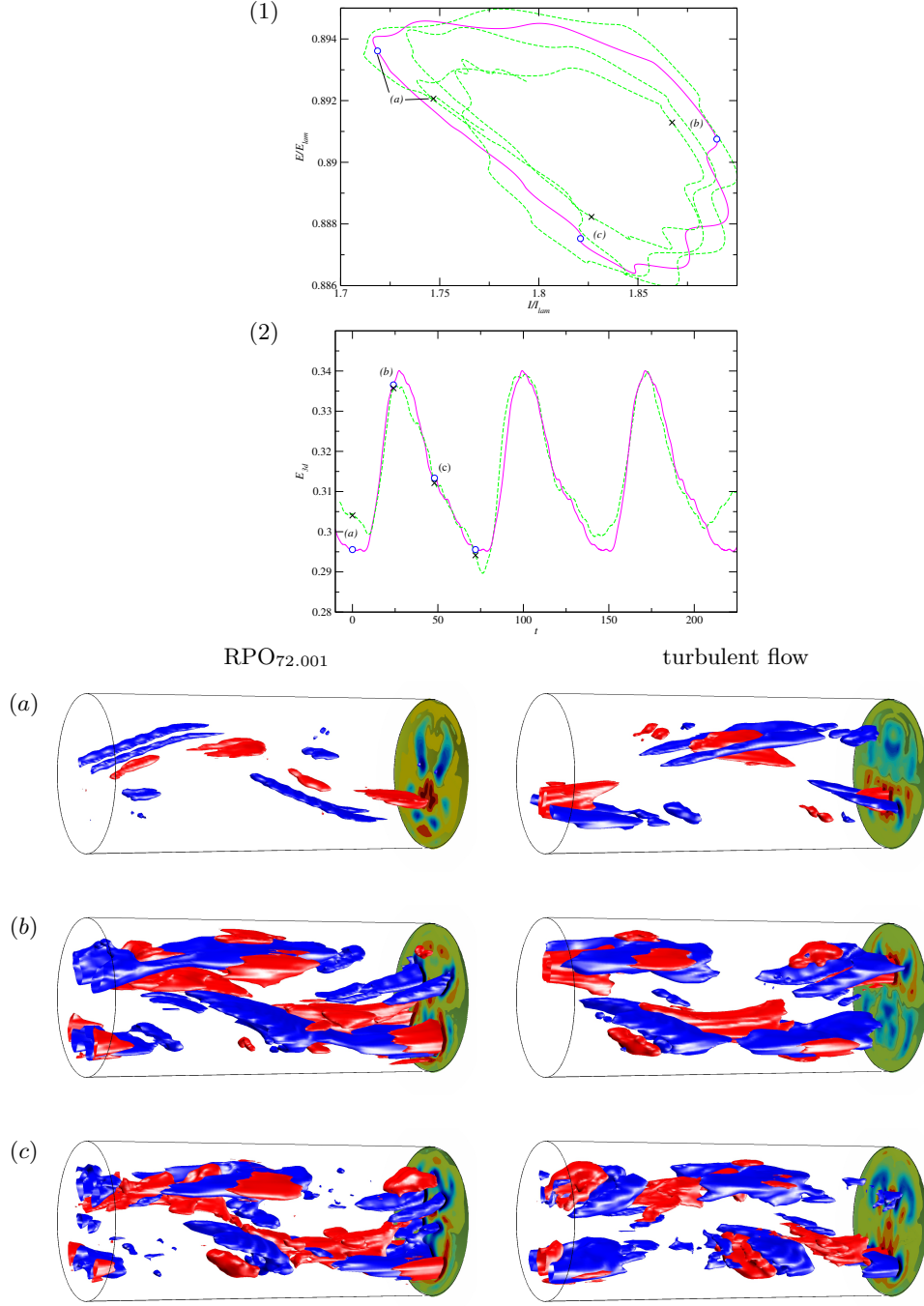


FIGURE 4. Evolution cycle of the spatio-temporal structures of $\text{RPO}_{72.001}$ ($T = 72.001$) and a turbulent flow hanging around it (for about three periods of $\text{RPO}_{72.001}$) in the bubble. The phases for the visualisation are identified by the symbols (a), (b), (c) in the phase plane (E, I) (1) and the monitored energy E_{3d} (2) (see also Figs. 1 and 2). Flow structures are visualised over one full cycle at three times with a constant interval about $24 t[D/U]$. Vortex structures are presented by isosurfaces of streamwise vorticity ω_z at $\pm 0.6 \max(\omega_z)$ (red (light gray) is positive and blue (dark gray) is negative) relative to the laminar flow for $\text{RPO}_{72.001}$ (left column) and nearby turbulent flow (right column) (From top to bottom they present snapshots of (a), (b) and the (c)). Color maps at right of each plot present corresponding cross sections (light (darker) indicate positive (negative) relative to the laminar flow.). See also online available material movie1.avi.

lifetime is dependent on the rate of switching (i.e. frequency of visits) to the bubble, rather than simply on the lifetime within the bubble itself. As a general picture, the state space is expected to be filled with a multitude of unstable invariant solutions, and turbulent trajectories visit the least unstable solutions. The long-period RPO and observations of shadowing manifests the perception that RPOs capture much of the natural measure of turbulent flows, within the subregion at least. Such RPOs are the most likely to be extracted directly from simulation. In future, the natural place to extend these ideas is to the larger domain, where localised structures such as puffs may exist. Work by Avila et al. (private communication (Results presented at EC565 meeting in Cargese 2014)) for lower Re but larger domains, appear to also be supportive. It is expected that the identification of RPOs will be a valuable tool in decoding natural characteristics of turbulence.

Acknowledgments

The research leading to these results has received funding from the Deutsche Forschungsgemeinschaft (Project No. FOR1182), and the European Research Council under European Union's Seventh Framework Programme (FP/2007-2013)/ERC Grant Agreement 306589. APW is supported by the EPSRC, grant EP/K03636X/1.

REFERENCES

- AVILA, M., MELLIBOVSKI, F., ROLAND, N. & HOF, B. 2013 Streamwise-localized solutions at the onset of turbulence in pipe flow. *Phys. Rev. Lett.* **110**, 224502.
- AVILA, M., WILLIS, A. P. & HOF, B. 2010 On the transient nature of localized pipe flow turbulence. *J. Fluid Mech.* **646**, 127–136.
- BUDANUR, N. B., CVITANOVIĆ, P., DAVIDCHACK, R. L. & SIMINOS, E. 2014 Reduction of $so(2)$ symmetry for spatially extended dynamical systems. *arXiv:1405.1096*.
- RESULTS PRESENTED AT EC565 MEETING IN CARGESE, CORSICA, FRANCE 2014.
- CHANTRY, M., WILLIS, A. P. & KERSWELL, R. R. 2014 Genesis of streamwise-localized solutions from globally periodic travelling waves in pipe flow. *Phys. Rev. Lett.* **112**, 164501.
- CVITANOVIĆ, P., ARTUSO, R., MAINIERI, G. TANNER & VATTAY, G. 2014 *Chaos: Classical and Quantum*. Niels Bohr Institute, Copenhagen: ChaosBook.org.
- CVITANOVIĆ, P. & GISON, J. F. 2009 *Advances in Turbulence XII: Geometry of turbulence in wall-bounded shear flows: periodic orbits*. Springer-Verlag Berlin Heidelberg: Springer Proceedings in Physics 132.
- DUGUET, Y., PRINGLE, C. C. T. & KERSWELL, R. R. 2008 Relative periodic orbits in transitional pipe flow. *Phys. Fluids* **20**, 114102.
- FAISST, H. & ECKHARDT, B. 2003 Traveling waves in pipe flow. *Phys. Rev. Lett.* **91**, 224502.
- HOF, B., CASIMIR, C. W. H., VAN DOORNE, WESTERWEEL, J., NIEUWSTADT, F. T. M., FAISST, H., ECKHARDT, B., WEDIN, H., KERSWELL, R. R. & WALEFFE, F. 2004 Experimental observation of nonlinear travelling waves in turbulent pipe flow. *Science* **305**, 1595.
- JIMÉNEZ, J., KAWAHARA, G., SIMENS, M., NAGATA, M. & SHIBA, M. 2005 Characterization of near-wall turbulence in terms of equilibrium and bursting solutions. *Phys. Fluids* **17**, 015105.
- KAWAHARA, G. 2005 Laminarization of minimal plane couette flow: going beyond the basin of attraction of turbulence. *Phys. Fluids* **17**, 041702.
- KAWAHARA, G. & KIDA, S. 2001 Periodic motion embedded in plane couette turbulence: regeneration cycle and burst. *J. Fluid Mech.* **449**, 291–300.
- KAWASAKI, M. & SASA, S. 2005 Statistics of unstable periodic orbits of a chaotic dynamical system with a large number of degrees of freedom. *Phys. Rev. E* **72**, 037202.
- KERSWELL, R. R. & TUTTY, O. R. 2007 Recurrence of travelling waves in transitional pipe flow. *J. Fluid Mech.* **584**, 69–102.

- KREILOS, T. & ECKHARDT, B. 2012 Periodic orbits near onset of chaos in plane couette flow. *Chaos* **22**, 4.
- KREILOS, T., ECKHARDT, B. & SCHNEIDER, T. M. 2014 Increasing lifetimes and the growing saddles of shear flow turbulence. *Phys. Rev. Lett.* **112**, 044503.
- MELLIBOVSKY, F. & ECKHARDT, B. 2011 Takens-bogdanov bifurcation of travelling wave solutions in pipe flow. *J. Fluid Mech.* **670**, 96–129.
- NAGATA, M. 1990 Three-dimensional finite-amplitude solutions in plane couette flow: bifurcation from infinity. *J. Fluid Mech.* **217**, 519–527.
- OKINO, S., NAGATA, M., WEDIN, H. & BOTTARO, A. 2010 A new nonlinear vortex state in square-duct flow. *Phys. Fluids* **657**, 413.
- PRINGLE, C. C. T., DUGUET, Y., & KERSWELL, R. R. 2009 Highly symmetric travelling waves in pipe flow. *Phil. Trans. Roy. Soc. Lond. A* **367**, 457.
- PRINGLE, C. C. T. & KERSWELL, R. R. 2007 Asymmetric, helical, and mirror-symmetric travelling waves in pipe flow. *Phys. Rev. Lett.* **99**, 074502.
- VISWANATH, D. 2007 Recurrent motions within plane couette turbulence. *J. Fluid Mech.* **580**, 339–358.
- VISWANATH, D. 2009 The critical layer in pipe flow at high reynolds number. *Phil. Trans. Roy. Soc. Lond. A* **367**, 561.
- WALEFFE, F. 2001 Exact coherent structures in channel flow. *J. Fluid Mech.* **435**, 93–102.
- WALEFFE, F. 2003 Homotopy of exact coherent structures in plane shear flows. *Phys. Fluids* **15**, 1517.
- WEDIN, H., BOTTARO, A. & NAGATA, M. 2009 Three-dimensional traveling waves in a square duct. *Phys. Rev. E* **79**, 065305.
- WEDIN, H. & KERSWELL, R. R. 2004 Exact coherent structures in pipe flow: travelling wave solutions. *J. Fluid Mech.* **508**, 333–371.
- WILLIS, A. P., CVITANOVIĆ, P. & AVILA, M. 2013 Revealing the state space of turbulent pipe flow by symmetry reductio. *J. Fluid Mech.* **721**, 514–540.
- WILLIS, A. P. & KERSWELL, R. R. 2009 Turbulent dynamics of pipe flow captured in a reduced model: puff relaminarisation and localised edge states. *J. Fluid Mech.* **619**, 213–233.